

### Introduction

Underwater acoustic research is a constantly growing area with ongoing improvements in measurement technologies. OceanSonics is an industry leader in the development of passively listening hydrophone devices (Fig. 1) which are widely used for biological and sonar technology research. These devices however suffer from unwanted noise created by their presence in moving flows; with the impact of the noise becoming more problematic for faster and faster flows. COMSOL Multiphysics 4.4, along with the CFD and acoustics module, was used in this study to better understand the turbulent and acoustic characteristics around and in the wake of the OceanSonics' hydrophones as fluid flows over it.



**Figure 1.** An OceanSonics iListen 3500 hydrophone and CAD model. Source: <http://oceansonics.com/iclisten-smart-hydrophones/>

### Computational Methods

The COMSOL  $k-\epsilon$  turbulence model was used to simulate flows up to 4 m/s (corresponding to  $Re < 30000$ ) over the hydrophone receiver. Model closure parameters were used to estimate the acoustic power (AP) generated by turbulent flow following [1]:

$$P = \alpha_\epsilon \rho \epsilon \frac{(2k)^{5/2}}{c^5}$$

Turbulent kinetic energy  $k$  and the dissipation rate  $\epsilon$  give the AP generated by the turbulence created by the hydrophone. The computational domain included a velocity inlet with minimal inherent turbulence and side walls moving to match the fluid velocity. COMSOL CAD and meshing tools were used to design the model. The mesh consisted of ~700,000 elements concentrated near regions of the hydrophone expected to generate the most turbulence. A 9 layer boundary mesh was applied to the surface of the hydrophone with a 1.15 stretching factor to ensure proper wall function application. The computational domain and hydrophone surface mesh are shown in Fig. 2.

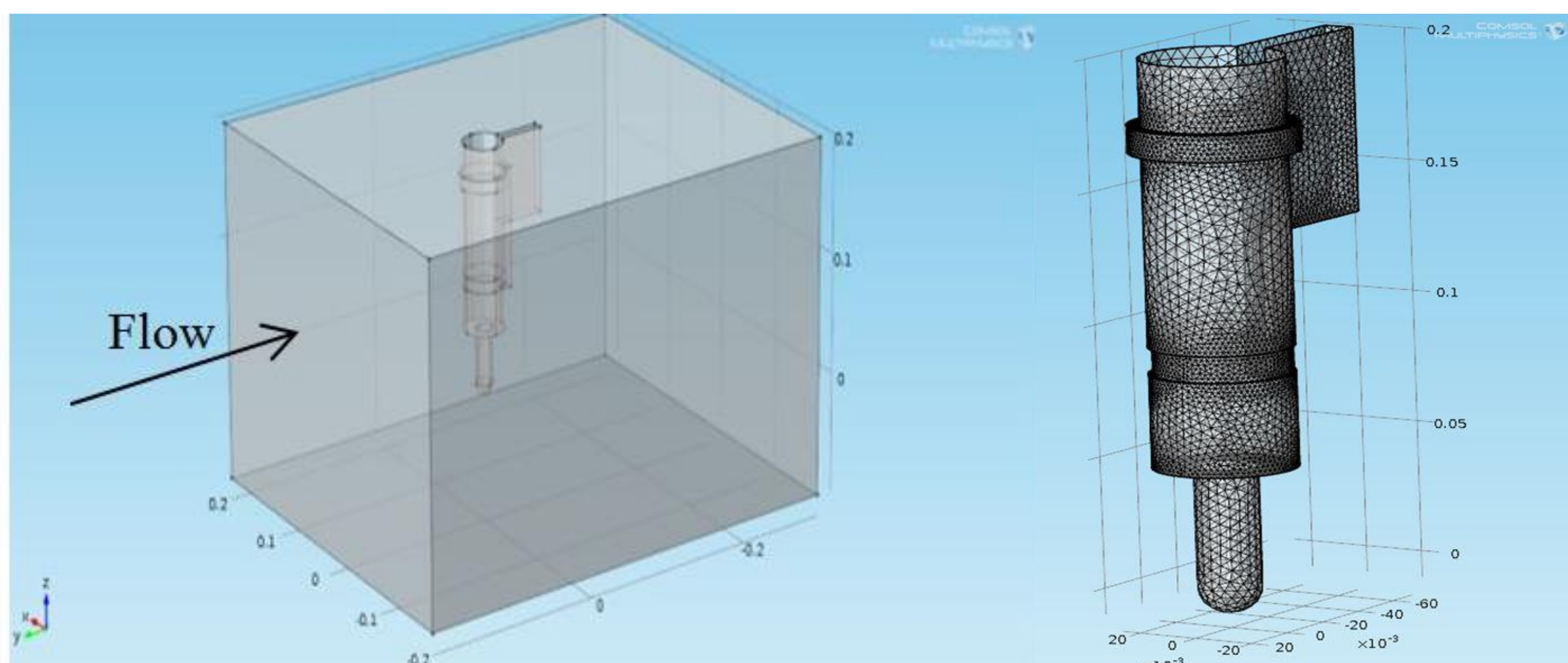


**Figure 2.** Model domain and surface mesh on the hydrophone

### Results

COMSOL simulations were run with free stream velocities up to 4 m/s. Flow field results show large velocity variations stemming from the diameter change between the thin base receiver and wide hydrophone body shown in Figs. 3 and 4.

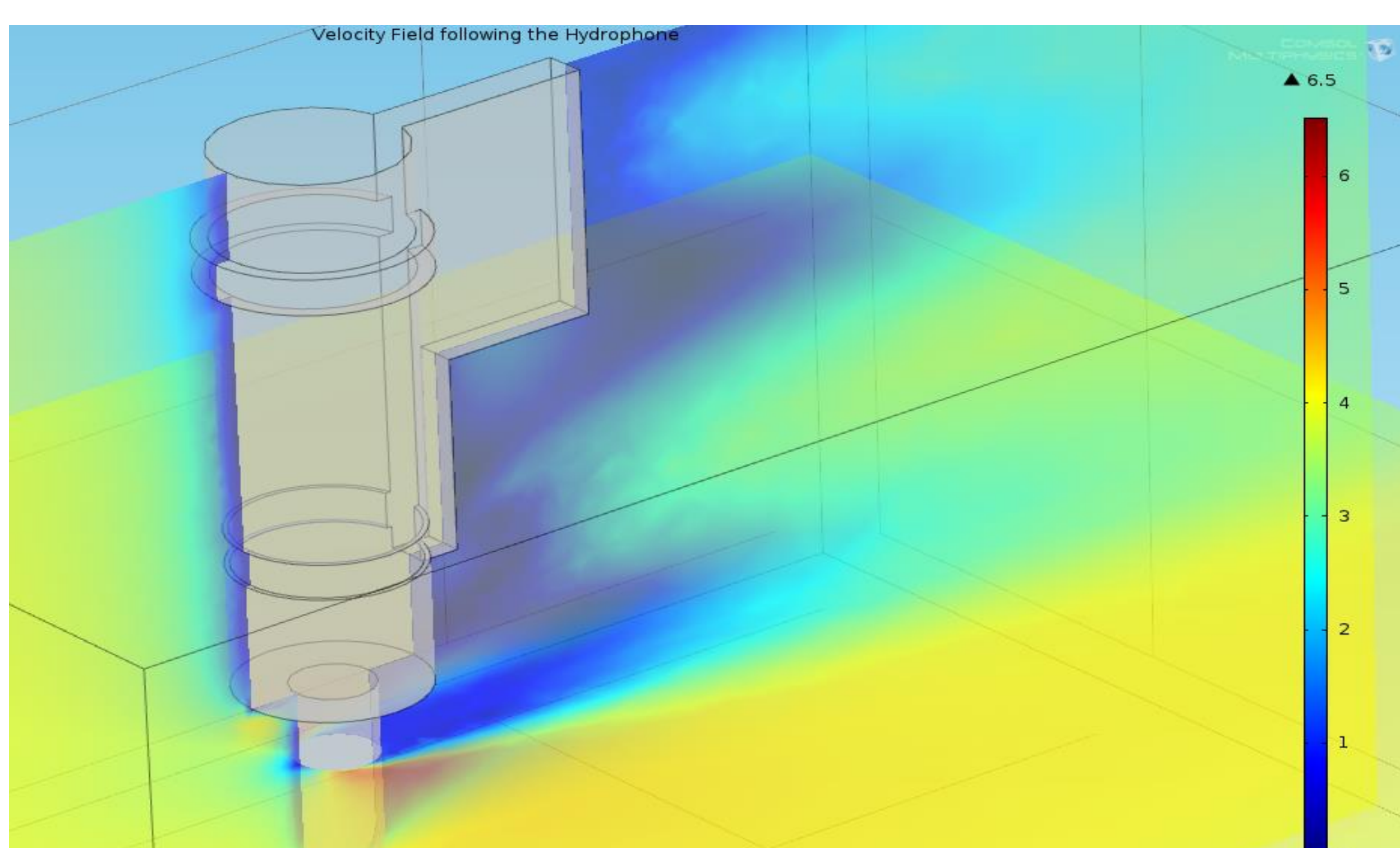


**Figure 3.** Flow field results of the wake following the hydrophone in 4 m/s free stream velocities.

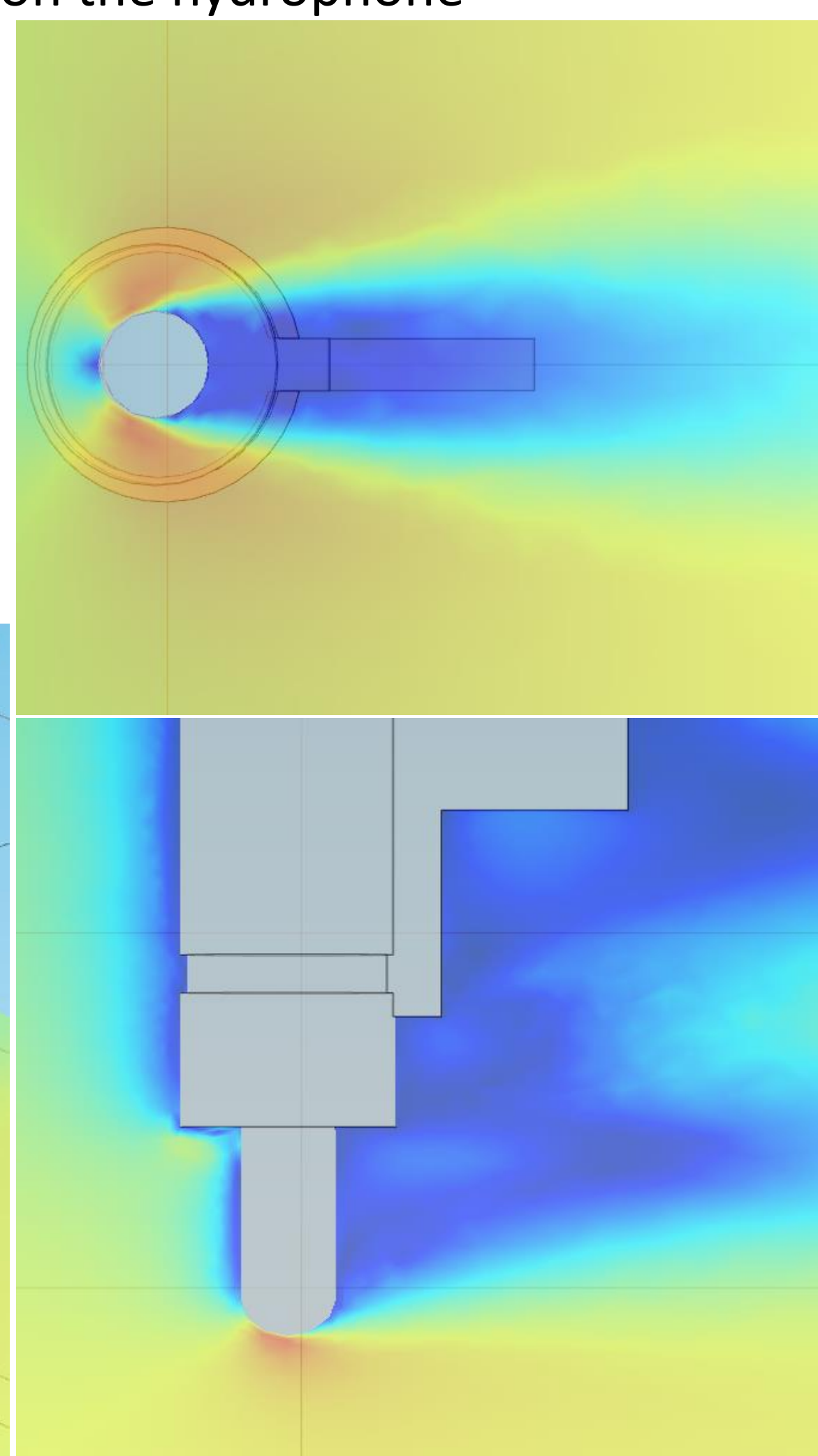


**Figure 4.** Velocity variations in the hydrophone wake viewed vertically along the hydrophone (top) and perpendicular to the flow direction (bottom).

The turbulent mixing between the hydrophone body and receiver contributes to the low frequency vibrations which are measured and can cause signal saturation at flow speeds  $> 3$  m/s. The COMSOL flow field results demonstrate a major contributor to this effect.

The AP generated in the wake of the hydrophone is shown in Figs. 5 and 6. Simulation results show the impact of the hydrophone diameter variations on the total AP in the wake in various flows.

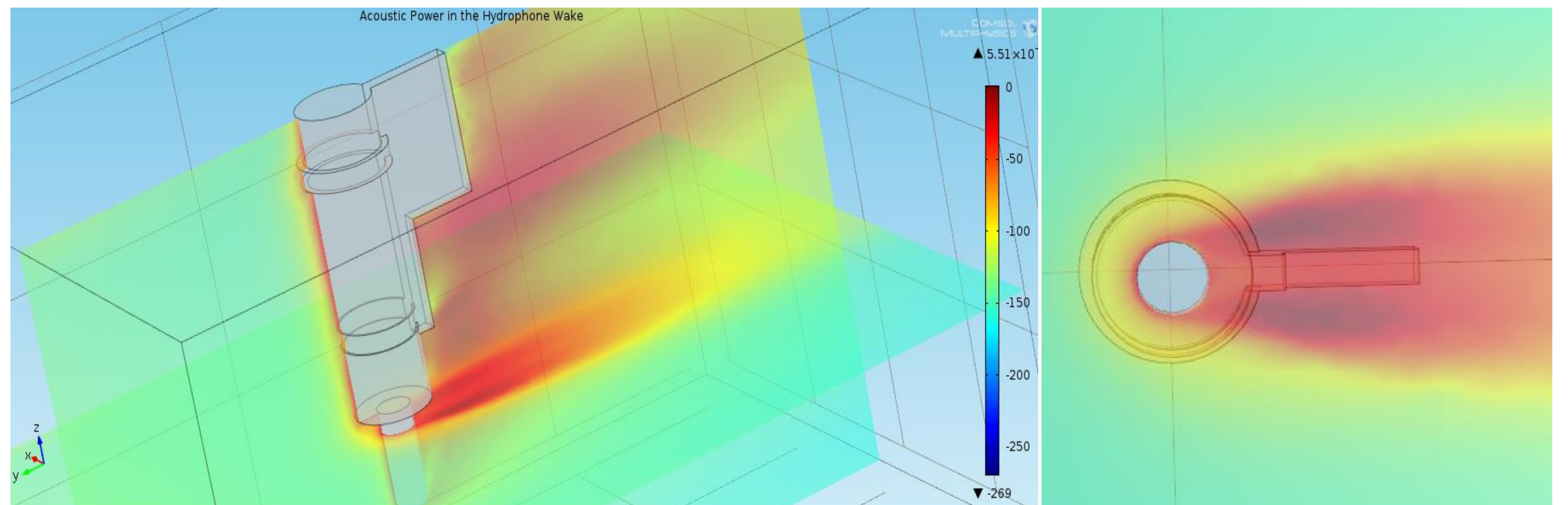
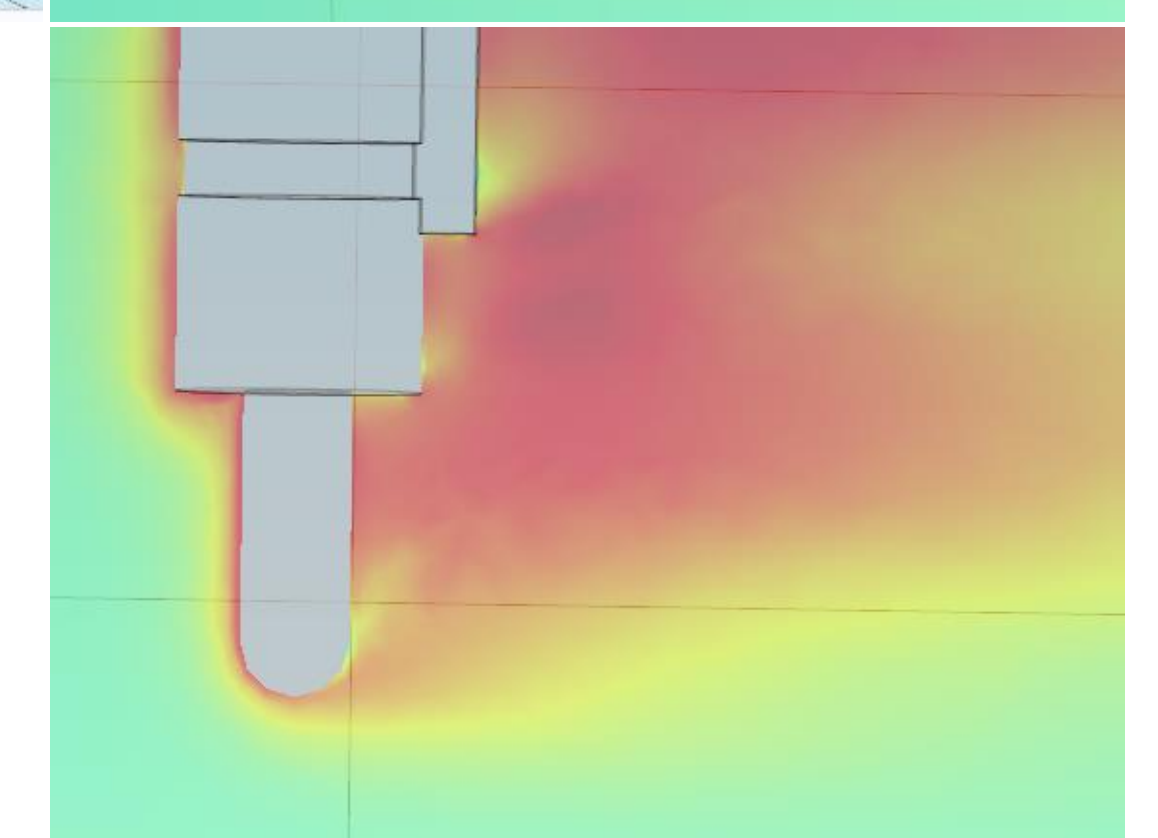


**Figure 5.** Acoustic Power in the wake following the hydrophone (dB).

Peak AP appears in the initial mixing region of flows passing the wide and thin diameter sections of the hydrophone. Maximum AP calculated reached  $3 \times 10^{-11}$  W/m<sup>3</sup> shown in Fig. 6.



The AP through the domain was calculated and statistically analyzed in Table 1 and Fig. 7. The AP distribution through the domain show the strength of acoustic noise in the wake.

**Table 1.** Acoustic power for various flow speeds.

Flow Speed	Mean	Standard Deviation	Maximum
1 m/s	$2.8 \times 10^{-17}$	$1.04 \times 10^{-16}$	$3.68 \times 10^{-15}$
2 m/s	$2.96 \times 10^{-15}$	$1.58 \times 10^{-14}$	$2.03 \times 10^{-12}$
3 m/s	$1.07 \times 10^{-13}$	$5.08 \times 10^{-13}$	$3.05 \times 10^{-11}$
4 m/s	$1.5 \times 10^{-13}$	$1.15 \times 10^{-12}$	$1.66 \times 10^{-11}$

The AP distribution through the wake shows that the strongest production regions of turbulent noise appear nearly 1 cm off of the back face of the receiver relative to the flow direction. The relative occurrence of AP increases with flow speed while the intensity appears to stabilize.

### Conclusions

Using COMSOL turbulence modelling software, the design features of the OceanSonics hydrophone leading to adverse acoustic noise have been quantified. Next steps in this study will include design changes to minimize the turbulence and acoustic noise to further improve the responsiveness of the device.

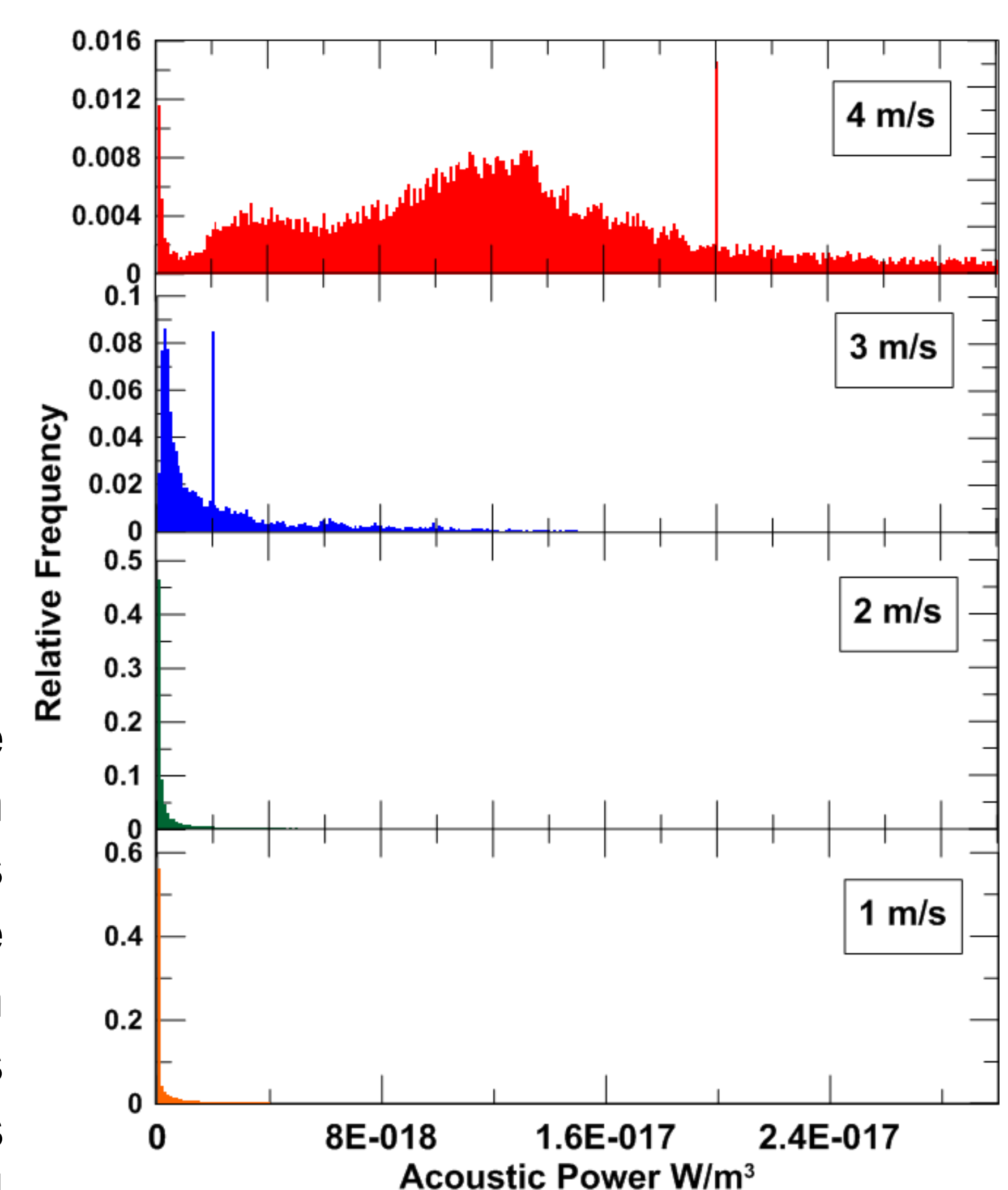


**Figure 7.** Acoustic power distributions.

### References:

1. I. Proudman, The generation of noise by isotropic turbulence, *Proc. R. Soc.*, **214**, 199-132 (1952).

### Acknowledgements

The authors are grateful to OceanSonics for their involvement in the development of this project as well as the Natural Science and Engineering Research Council of Canada (NSERC) through their ENGAGE program and the Canadian Foundation for Innovation (CFI) for their financial assistance.